Self-trapped quantum walks

A. R. C. Buarque and W. S. Dias
Instituto de Física, Universidade Federal de Alagoas, 57072-900 Maceió, Alagoas, Brazil

(Received 22 October 2019; accepted 10 January 2020; published 4 February 2020)

We study the existence and characterization of self-trapping phenomena in discrete-time quantum walks. By considering a Kerr-like nonlinearity, we associate an acquisition of the intensity-dependent phase with the walker while it propagates on the lattice. Adjusting the nonlinear parameter χ and the quantum gates θ, we will show the existence of different quantum walking regimes, including those with traveling solitonlike structures or localized by self-trapping. The latter scenario is absent for quantum gates close enough to the Pauli-X gate. It appears for intermediate configurations and becomes predominant as quantum gates get closer to the Pauli-Z gate. By using χ versus θ diagrams, we will show that the threshold between quantum walks with delocalized or localized regimes exhibits an unusual aspect in which an increment of the nonlinear strength can induce the system to transition from a localized to a delocalized regime.

DOI: 10.1103/PhysRevA.101.023802

I. INTRODUCTION

Quantum-mechanical systems in which the effective evolution is governed by a nonlinear equation are present in many branches of science such as optics [1–3], biology [4,5], Bose-Einstein condensates [6–8], and solid-state physics [9–12]. In optical media, for example, nonlinearity arises from field-induced changes in the refractive index of the propagation medium [1–3], while for Bose-Einstein condensates the nonlinearity is related to interatomic interactions [6–8]. Nonlinearity also appears as a result of lattice vibrations in the dynamic description of elementary excitations [4,5,9–12].

Among the most interesting subjects related to nonlinearity are the self-trapping states. When associated with delocalized modes, initial excitations display as a signature propagation without spreading (shape preserving), due to a balance between nonlinearity and linear correlation (dispersion, diffraction, and diffusion) effects [1,3–5,7–20]. However, the absence of propagation is also a remarkable effect of self-trapping states. In this case, an initial excitation is induced to trapping, with a significant time-averaged probability of finding it in a finite region of the system when the nonlinear coupling is above a threshold value [21–29].

Both scenarios have been widely studied in different areas. In the context of optical fibers, for example, the employment of solitonlike features for optical communications has been studied [13–16]. Soliton and solitonlike structures have also been reported as underlying mechanisms of charge carrier transport of conducting polymers [11,12,18–20]. Self-trapped vortex beams azimuthally stable at moderate values of the input intensity have been reported, in which the saturation of the refractive nonlinearity and the instability-suppressing effect of the three-photon absorption display a fundamental role [24]. Driven-dissipative Bose-Einstein condensates (BECs) in a two-mode Josephson system have been used to obtain the alternating current Josephson effect with magnons as well as macroscopic quantum self-trapping in a magnon BEC [28].

Although nonlinear aspects have been reported in the context of discrete-time quantum walks (DTQWs), a full understanding of the phenomenology is still distant. One of the earliest studies that reported a nonlinear self-phase modulation on the wave function during the walker evolution showed the formation of nondispersive pulses [30]. An anomalous slow diffusion has been reported for a nonlinear quantum walk in which the coin operator depends on the coin states of the nearest-neighbor sites [31]. The dynamics of a nonlinear Dirac particle has been simulated by using a nonlinear quantum walk, with a description of solitonic behavior and the collisional phenomena between them [32]. By using DTQWs which combine zero modes with a particle-conserving nonlinear relaxation mechanism, a conversion of two zero modes of opposite chirality into an attractor-repeller pair of nonlinear dynamics was reported [33]. By investigating the effect of nonlinear spatial disorder on the edge states at the interface between two topologically different regions, the preservation of the ballistic propagation of the walker has been described even for very strong nonlinear couplings [34]. Nonlinear effects on the quantum walks ruled by Pauli-X gates homogeneously distributed have revealed the existence a set of stationary and moving breathers with almost compact superexponential spatial tails [35]. Disordered nonlinear DTQWs were used to confirm that the subdiffusive spreading of wave packets (well known in Gross-Pitaevskii lattices) persists over an additional four decades, which suggests that this subdiffusive behavior is universal [36]. Cross Kerr nonlinearity and orbital angular momentum have been used as two distinct degrees of freedom in the position space in order to propose a scheme able to perform infinite steps of two-dimensional DTQWs [37].

A quantum walk is known to be usually faster than its classical counterpart due to coherent superposition and quantum interference [38,39]. This feature makes it a versatile tool for the realization of quantum algorithms and quantum simulation [39–41]. In this context, the number of studies on quantum computation based on optics is growing, in which

the left and right polarization states of a single photon make up a natural computational basis of qubits. Thus, motivated by the wide nonlinear phenomenology in optical systems, we investigate the dynamics of quantum walkers in nonlinear DTQWs. Different from nonlinear feedforward DTQWs [31], we associate the acquisition of the intensity-dependent phase with the walker while it propagates on the lattice. This nonlinear phase, together with each of the spinor components, may be the result of a Kerr-like optical medium in the optical paths. With the nonlinearity described by adding an operator to the standard protocol of DTQWs [30,42], we study the transport properties by exploring typical quantities such as the inverse participation ratio, the survival probability, and the wave-function profile. Keeping in mind Ref. [30], which presented a preliminary study restricted to Hadamard's quantum gates only, we explore the adjustment of the nonlinear parameter and quantum gates to show the existence of different quantum walking regimes, including those with traveling solitonlike structures or localized by self-trapping. In the latter, the dispersive mode is fully suppressed by nonlinearity, making the walker strongly trapped in the initial position, developing a breathing mode. This scenario is absent for quantum gates close enough to the Pauli-X gate. It appears for intermediate configurations and becomes predominant as quantum gates get closer to the Pauli-Z gate. The threshold between quantum walks with delocalized or localized regimes exhibits an unusual aspect in which an increment of the nonlinear strength can induce the transition of the system from a localized to a delocalized regime.

II. MODEL

In this work we deal with a quantum walker moving in an infinite one-dimensional nonlinear lattice of interconnected sites. The walker consists of a qubit whose internal degree of freedom (spin or polarization) determines the direction of movement in discrete steps. Thus, the quantum walker state $|\psi\rangle$ belongs to a Hilbert space $H = H_c \otimes H_p$, where H_c is a complex vector space of dimension 2 associated with the internal degree of freedom of the qubit and H_p denotes a countably-infinite-dimensional space associated with lattice sites. We describe the internal degree of freedom spanned by orthonormal basis $\{|R\rangle = (1,0)^{\mathsf{T}}, |L\rangle = (0,1)^{\mathsf{T}}\}$, where the superscript denote transpose, in Hilbert space H_c. The position space H_p is spanned by the orthonormal basis $\{|n\rangle : n \in \mathbb{Z}\}$, with n ranging from $n = 1$ to N. Thus, a general state in the tth time step can be given as

$$|\psi(t)\rangle = \sum_n [a(n,t)|R\rangle + b(n,t)|L\rangle] \otimes |n\rangle, \tag{1}$$

so the normalization condition $\sum_n [|a(n,t)|^2 + |b(n,t)|^2] = 1$ is satisfied.

In general, the dynamical evolution of a discrete-time quantum walk is governed by the unitary transformation $|\psi(t)\rangle = \hat{U}^t|\psi(t-1)\rangle$, where $\hat{U}^t = \hat{S}(\hat{C} \otimes I_P)$, with I_P the identity operator in the space of positions. The conditional shift operator has the form

$$\hat{S} = S_+ \otimes |R\rangle\langle R| + S_- \otimes |L\rangle\langle L|, \tag{2}$$

where $S_\pm = \sum_{n=1}^{N} |n \pm 1\rangle\langle n|$, while $\hat{C}$ (well known as a quantum coin) is an arbitrary SU(2) unitary operator given by

$$\hat{C} = \sum_n [c_{R,R}|R\rangle + c_{L,R}|L\rangle]\langle R| + [c_{R,L}|R\rangle - c_{L,L}|L\rangle]\langle L| \otimes |n\rangle\langle n|, \tag{3}$$

with $c_{R,R} = c_{L,L} = \cos(\theta)$ and $c_{R,L} = c_{L,R} = \sin(\theta)$. The parameter $\theta \in [0, 2\pi]$ controls the variance of the probability distribution of the walk [43].

Here, in order to introduce the nonlinearity, we add to the dynamical evolution protocol one more operator that describes the acquisition of an intensity-dependent (nonlinear) phase by each of the spinor components [30]. Thus, $\hat{U}^t = \hat{S}(\hat{C} \otimes I_P)\hat{U}_{NL}^{t-1}$, where $\hat{U}_{NL}$ is given by

$$\hat{U}_{NL}^t = \sum_{s=R,L} \sum_n e^{iG^t(n,s)} |s\rangle\langle s| \otimes |n\rangle\langle n| = \sum_n (e^{iG^t(n,R)}|R\rangle\langle R| + e^{iG^t(n,L)}|L\rangle\langle L|) \otimes |n\rangle\langle n|. \tag{4}$$

Here $G^t(n,s)$ is an arbitrary function of the probabilities, depending on the internal degree of freedom (coin state) and the lattice site (spatial state).

We consider the experimental implementation feasible by inserting nonlinear optical media into optical setups able to describe DTQWs, such as a linear cavity [44], optical rings [45–47], a Michelson interferometer [48], or optical lattices [49]. By considering a Kerr-like nonlinearity, we set $G^t(n,s) = 2\pi\chi|\psi_{n,s}^t|^2$, in which χ describes the nonlinear strength of the medium and the linear discrete-time quantum walk can be recovered by setting $\chi = 0$. By using the time-evolution protocol $|\psi(t)\rangle = \hat{U}^t|\psi(t-1)\rangle$ we can derive the recursive evolution equations for the probability amplitudes

$$\begin{aligned} \psi_{n,R}^{t+1} &= c_{R,R} e^{i2\pi\chi|\psi_{n+1,R}^t|^2} \psi_{n+1,R}^t + c_{R,L} e^{i2\pi\chi|\psi_{n+1,L}^t|^2} \psi_{n+1,L}^t, \\ \psi_{n,L}^{t+1} &= c_{L,R} e^{i2\pi\chi|\psi_{n-1,R}^t|^2} \psi_{n-1,R}^t - c_{L,L} e^{i2\pi\chi|\psi_{n-1,L}^t|^2} \psi_{n-1,L}^t. \end{aligned} \tag{5}$$

Thus, the state of the quantum particle in the tth time step is given by the two-component wave function $\{\psi_{n,R}^t, \psi_{n,L}^t\}$, where $\psi_{n,R}^t$ and $\psi_{n,L}^t$ are the probability amplitudes of obtaining the states $|R\rangle$ and $|L\rangle$ at position n and time step t, respectively. We consider throughout the analysis open chains as the boundary condition, in which the initial position n_0 of the quantum walker is located in the central site of the lattice. We emphasize that the lattice sizes are large enough so that the wave function does not reach the edges over the time course described.

III. RESULTS AND DISCUSSION

We start following the time evolution of the probability density distribution $|\psi_n(t)|^2$ for some representative values of the nonlinear parameter χ. With the initial state of the walker adjusted as a superposition of left- and right-handed circular polarization $[|\Psi(0)\rangle = 1/\sqrt{2}(|R\rangle + i|L\rangle) \otimes |n_0\rangle]$, we show in Fig. 1 the dynamics described in chains ruled by quantum gates $\theta = \pi/4$ [Figs. 1(a)–1(d)] and $\theta = \pi/3$ [Figs. 1(e)–1(h)] homogeneously distributed. As expected, in the absence of nonlinearity ($\chi = 0.0$) both quantum gates induce a spread of the probability distribution through the lattice, exhibiting

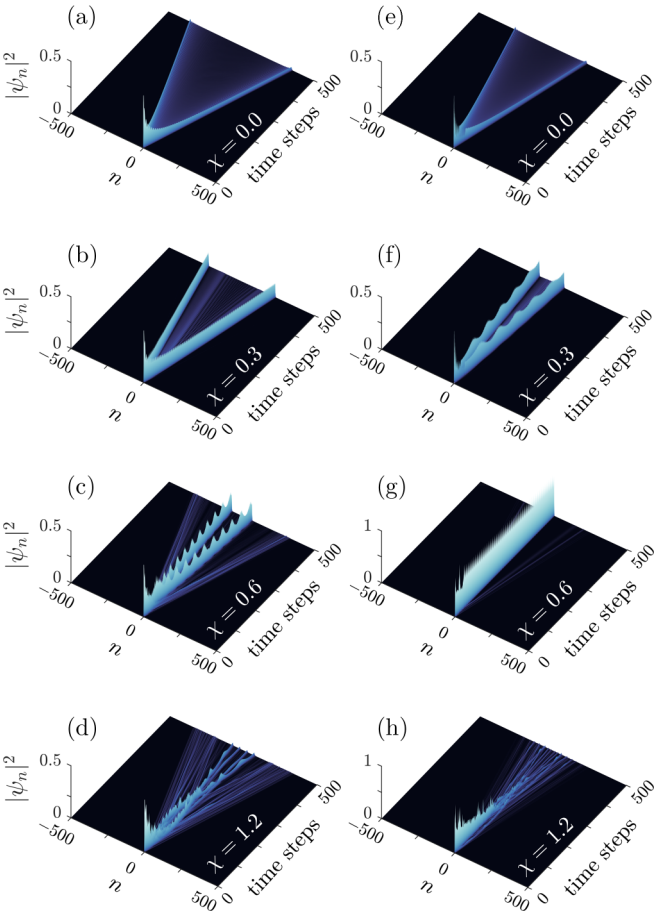

FIG. 1. Time evolution of the density of probability in position space of a quantum walker on chains composed of quantum gates (a)–(d) $\theta = \pi/4$ and (e)–(h) $\theta = \pi/3$ homogeneously distributed. Both quantum gates exhibit traveling solitonlike structures in the presence of nonlinearity, whose velocity decreases as the nonlinear parameter χ increases. Although both scenarios culminate in a scenario of collisions with inelastic scattering for sufficiently strong nonlinearities, a self-trapped quantum walk emerges only for $\theta = \pi/3$, which suggests a phenomenology with gate dependence.

two peaks at the borders of the distribution, whose maximum value monotonically decreases with time. However, this scenario is heavily altered as χ grows. For $\chi = 0.3$, we observe the probability distribution predominantly concentrated at a few lattice positions, by establishing two mobile peaks whose size and shape remain approximately constant in time, except for small oscillations around a mean value. Traveling self-trapped states are consistent with the observation of solitonlike structures described in Ref. [30] and also have been reported in other systems [17,50]. The results of Hadamard quantum gates ($\theta = \pi/4$) suggest that the velocity of the solitonlike formations decreases as χ increases in such way that, for sufficiently strong nonlinearities, a scenario of collisions with inelastic scattering arises. However, as we increase the nonlinear parameter for the system ruled by $\theta = \pi/3$, a different behavior is observed. For $\chi = 0.6$ the probability distribution remains predominantly trapped around the initial position, i.e., a stationary self-trapped quantum walk. Furthermore, contrary to expectation, the concentration of the

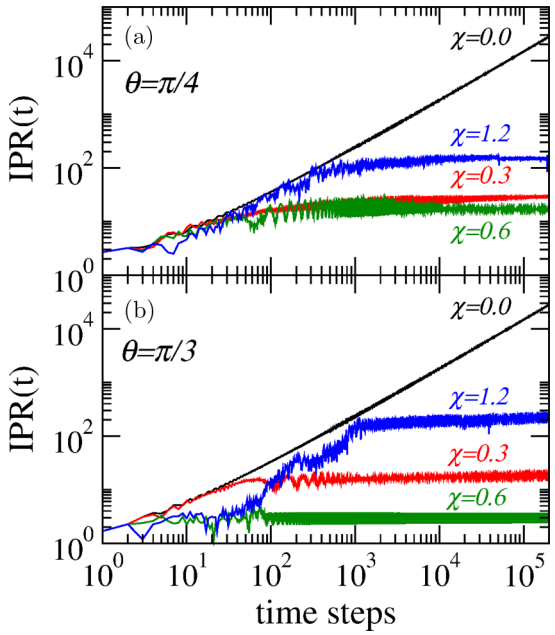

FIG. 2. Time evolution of the inverse participation ratio for the same configurations used in Fig. 1. We observe the IPR(t) recovering relevant aspects reported before, from the standard quantum walk ($\chi = 0$) to the self-trapped quantum walk ($\theta = \pi/3$ with $\chi = 0.6$).

walker around the initial position does not grow as χ increases. Just like $\theta = \pi/4$, collisions with inelastic scattering arise for sufficiently strong nonlinearities.

In order to better characterize the previous results we compute the inverse participation ratio

$$\mathrm{IPR}(t) = \frac{1}{\sum_n |\psi_n(t)|^4}, \tag{6}$$

which gives the estimated number of lattice sites over which the wave packet is spread at time t. Thus, in Fig. 2 we use the same configurations shown in Fig. 1, with Figs. 2(a) and 2(b) describing the systems ruled by quantum coins $\theta = \pi/4$ and $\theta = \pi/3$, respectively. We see that IPR(t) recovers relevant aspects reported before. While the spread of the quantum walker is described by IPR(t) growing over time in the absence of nonlinearity, the dynamics involving solitonlike structures (for $\chi = 0.3, 0.6, 1.2$) is described by IPR(t) approximately constant after an initial transient. The lower inverse participation ratio for $\theta = \pi/3$ and $\chi = 0.6$ corroborates the localization induced by self-trapping phenomena described above. On the other hand, multiple collisions between solitonlike structures induce a walker scattering, which explains the behavior of $\chi = 1.2$.

We achieve a complementary analysis by computing the survival probability

$$\mathrm{SP}(t) = \sum_{s=R,L} |\langle n| \otimes \langle s|\psi(t)\rangle|^2 \Big|_{n=n_0}. \tag{7}$$

This quantity describes the probability of the walker being found at the starting position at time t. In the long-time regime the survival probability saturates at a finite value for

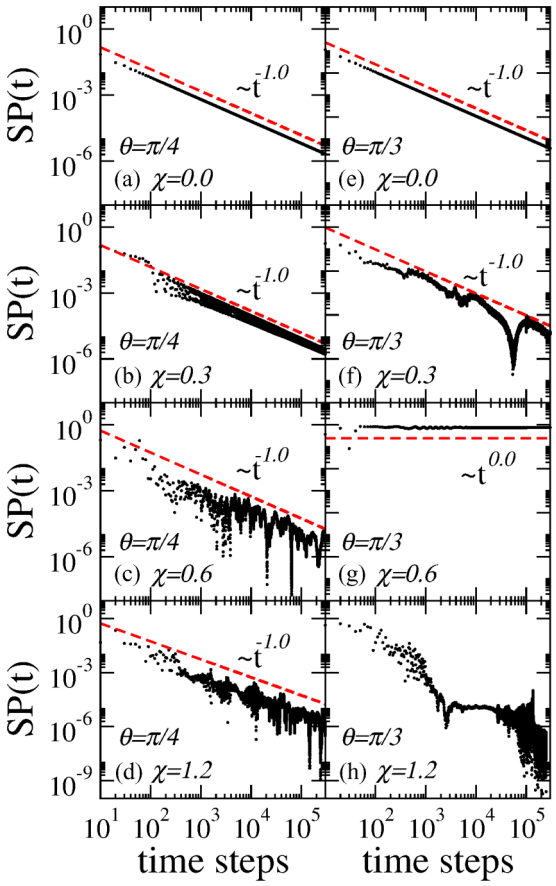

FIG. 3. Time evolution of the survival probability for the same configurations used in Fig. 1. We observe the SP(t) confirming all aspects reported before. The scaling behavior SP(t) $\sim t^{-1}$, which is well defined for almost all configurations, gives way to SP(t) $\sim t^{0}$ for $\theta = \pi/3$ with $\chi = 0.6$, which corroborates a self-trapped quantum walk.

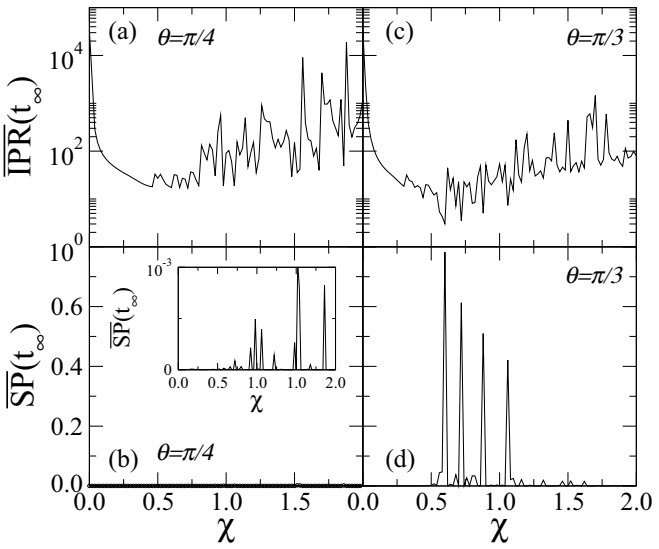

FIG. 4. Long-time average of the inverse participation ratio and survival probability versus the nonlinear parameter χ for quantum gates $\theta = \pi/4$ and $\theta = \pi/3$. Both quantities agree with the existence of traveling solitonlike structures for sufficiently small nonlinearities and with a chaoticlike regime for sufficiently strong nonlinearities. However, the emergence of χ settings for $\theta = \pi/3$ in which $\overline{\mathrm{IPR}}(t_\infty)$ and $\overline{\mathrm{SP}}(t_\infty)$ are close to unity corroborates the quantum walker localization by self-trapping, as well as its gate dependence.

a localized quantum walk, while SP(t) $\to 0$ means that the walker is escaping from its initial location.

In Fig. 3 we show the time evolution of SP(t) for the same configurations used before, with Figs. 3(a)–3(d) [Figs. 3(e)–3(h)] giving $\theta = \pi/4$ ($\theta = \pi/3$). In the absence of nonlinearity, the spreading of the walker on the lattice is described by a scaling behavior SP(t) $\sim t^{-1}$, which is in full agreement with an explicit expression in Ref. [51]. We also observe this scaling behavior for $\theta = \pi/4$ and $\chi = 0.3, 0.6, 1.2$, which is consistent with solitonlike modes traveling through the lattice, i.e., the absence of the walker localization. On the other hand, for $\theta = \pi/3$ another pattern is revealed: For $\chi = 0.6$ we have SP(t) $\sim t^{0}$ after an initial transient, which describes the walker remaining localized around its initial position. In agreement with Fig. 2, SP(t) close to unity for $\chi = 0.6$ [see Fig. 3(g)] reinforces the idea of stationary trapping. In addition, SP(t) decreasing for $\chi = 1.2$ confirms the absence of walker localization at the initial site after a long time evolution. The roughness in SP(t) data suggests destructive interferences of solitonlike structures as time evolves.

Previous results suggest the regime of localized self-trapped quantum walks as gate dependent, i.e., restricted to some configurations of quantum gates. This behavior is consistent with the dispersive character associated with the distribution of quantum gates on the lattice [52], since the emergence and dynamics of solitonlike structures are associated with balancing between nonlinearity and linear correlation (dispersion, diffraction, and diffusion) effects [1,3–5,7–20]. In order to provide a broader and accurate description, we explore the asymptotic regime of IPR(t) and SP(t) for distinct θ settings. We keep considering infinite lattices, but now we compute the average of both quantities around 10^4 time steps, identified by $\overline{\mathrm{IPR}}(t_\infty)$ and $\overline{\mathrm{SP}}(t_\infty)$. In Fig. 4 we explore $\theta = \pi/4$ and $\theta = \pi/3$ for a range of the nonlinear parameter χ between 0 and 2. For the early stage of nonlinearity, both $\overline{\mathrm{IPR}}(t_\infty)$ and $\overline{\mathrm{SP}}(t_\infty)$ suggest delocalized quantum walks in which the walker spreads out on the lattice. Mobile solitonlike structures arise as χ grows, described by the decrease in $\overline{\mathrm{IPR}}(t_\infty)$ and $\overline{\mathrm{SP}}(t_\infty) \sim 0$. The emergence of χ settings for $\theta = \pi/3$ in which $\overline{\mathrm{IPR}}(t_\infty)$ and $\overline{\mathrm{SP}}(t_\infty)$ are close to unity, corroborates the quantum walker localization by self-trapping, as well as its gate dependence. For sufficiently strong nonlinearities, a chaoticlike regime has been found not only for $\theta = \pi/4$ [30], but also for $\theta = \pi/3$. Here the walker dynamics becomes extremely sensitive to small variations of the nonlinear parameter. This regime comprises quantum walks with delocalized solitonlike structures (where modes are continuously moving apart) and solitonlike dynamics with multiple modes and collisions. This chaoticlike behavior has been shown in other nonlinear systems [17,50].

For Fig. 5 we extend our numerical experiments in order to offer χ versus θ diagrams. In Fig. 5(a) we consider the maximal IPR between collected data in order to plot on the vertical axis a normalized $\overline{\mathrm{IPR}}(t_\infty)$. For Fig. 5(b) we compute the $\overline{\mathrm{SP}}(t_\infty)$ as before. The initial state of the walker is again

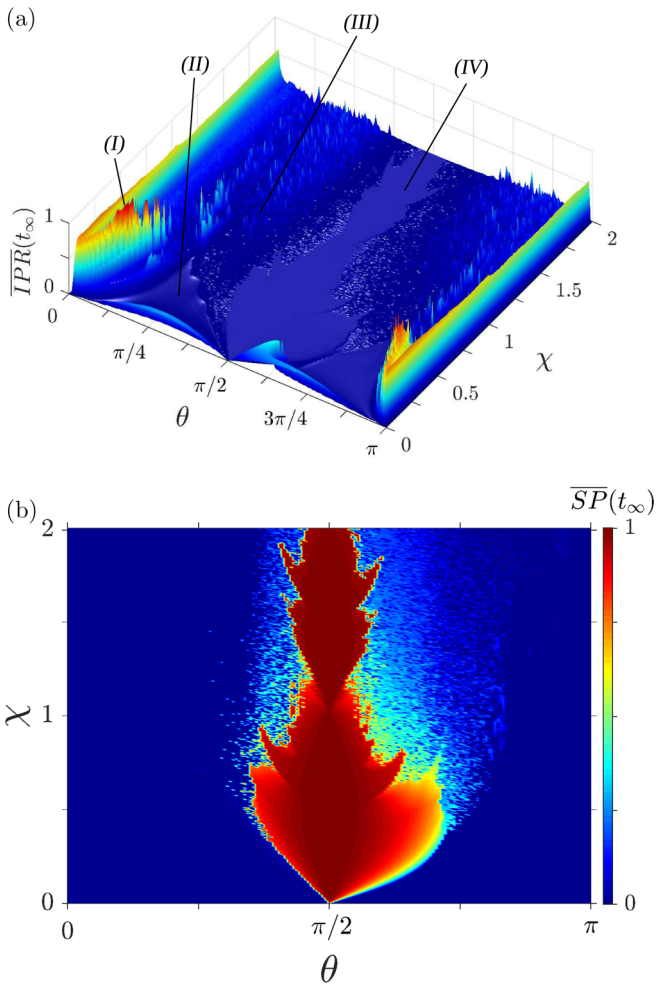

FIG. 5. Plot of χ versus θ for the long-time average of the inverse participation ratio and the survival probability. The initial state of the walker is again described as a superposition of left- and right-handed circular polarization, i.e., $|\Psi(0)\rangle = 1/\sqrt{2}(|R\rangle + i|L\rangle) \otimes |n_0\rangle$, with the initial position n_0 of the quantum walker located at the central site of the lattice. We note the absence of trapped structures for sufficiently small θ values, even for a strong nonlinear parameter (I). As we increase θ toward $\pi/2$, different scenarios emerge as we change the χ value: (II) solitonlike structures propagating through the lattice, (III) a chaoticlike regime, and (IV) stationary self-trapped quantum walks.

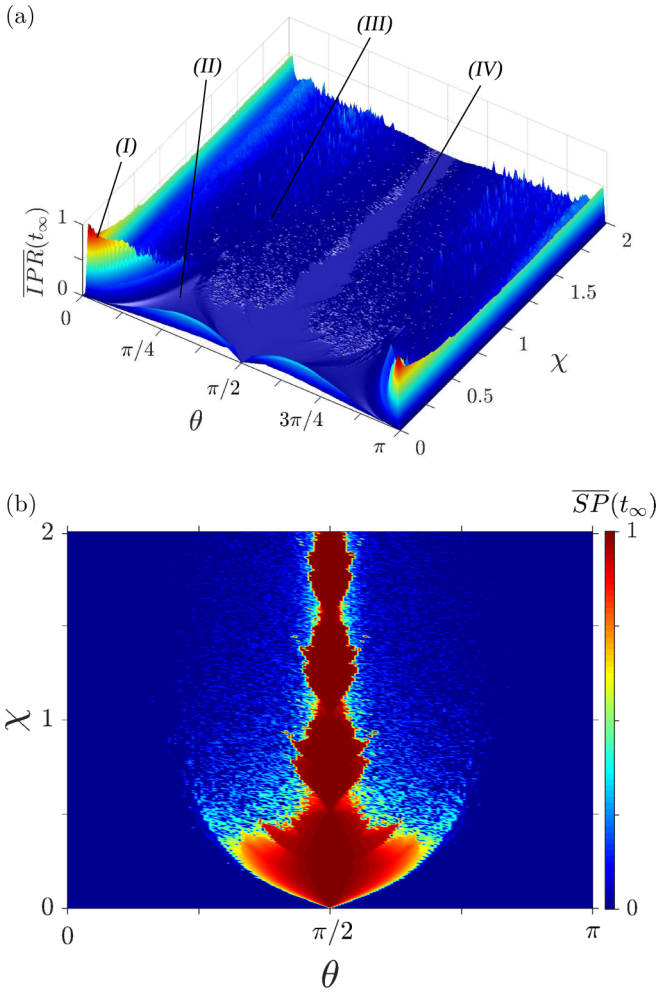

FIG. 6. Plot of χ versus θ for the long-time average of the inverse participation ratio and the survival probability. The initial state of the walker now is given by $|\Psi(0)\rangle = |R\rangle \otimes |n_0\rangle$, with the initial position n_0 of the quantum walker located at the central site of the lattice. In general, the phenomenology is homologous to behavior described by the initial state $|\Psi(0)\rangle = 1/\sqrt{2}(|R\rangle + i|L\rangle) \otimes |n_0\rangle$. However, we observe now a symmetric profile around $\theta = \pi/2$ and the regime of stationary self-trapped quantum walks is even more concentrated around $\theta = \pi/2$.

described as a superposition of left- and right-handed circular polarization, i.e., $|\Psi(0)\rangle = 1/\sqrt{2}(|R\rangle + i|L\rangle) \otimes |n_0\rangle$, with the initial position n_0 of the quantum walker located in the central site of the lattice. By simultaneously exploring both diagrams, we note the absence of trapped structures for sufficiently small θ values, even for a strong nonlinear parameter. In this regime (I), the dispersive character is predominant, with a small contribution from the interference terms of the $\hat{C}$ matrix. Moreover, in this regime, the increase of $\overline{\mathrm{IPR}}(t_\infty)$ suggests the nonlinearity as a mechanism able to increase the spread of the walker. However, this behavior is not related to the spreading velocity, but rather to the wave-function distribution, which now exhibits a more uniform profile than the one presented in the absence of nonlinearity. The wavefronts exhibit aspects close to a solitonlike structure, but decrease slowly with time.

As we increase θ toward $\pi/2$, different scenarios emerge as we change the χ value. For χ sufficiently small, the normalized $\overline{\mathrm{IPR}}(t_\infty) \sim 0$ with $\overline{\mathrm{SP}}(t_\infty) \sim 0$ is consistent with the existence of solitonlike structures propagating through the lattice (II). As described before (see Fig. 4), the increase of χ promotes a regime in which the evolution of the solitons becomes extremely sensitive to small variations of the nonlinear parameter (III). This behavior is found for high enough χ values and is described by fluctuations of the normalized $\overline{\mathrm{IPR}}(t_\infty)$ and $\overline{\mathrm{SP}}(t_\infty)$. Stationary self-trapped quantum walks (IV) become evident as we observe the normalized $\overline{\mathrm{IPR}}(t_\infty) \sim 0$ and $\overline{\mathrm{SP}}(t_\infty) \sim 1$. Both diagrams confirm that, once within a stationary self-trapped regime, an increment of χ does not mean an increase of the localization degree. Thus, the threshold between delocalized and localized regimes exhibits an unusual aspect. We also observe the stationary self-trapped

regime becoming predominant as θ gets closer to Pauli-Z quantum gates ($\theta = \pi/2$). In this configuration, whose energy spectrum of the two main bands resembles that of flat degenerate bands [52], the dynamics that transitions $|R\rangle$ to $|L\rangle$ and $|L\rangle$ to $|R\rangle$ is reinforced by the nonlinear (probability-dependent) phase.

A characteristic absent in the previous discussion is the asymmetric aspect of the normalized $\overline{\mathrm{IPR}}(t_\infty)$ and $\overline{\mathrm{SP}}(t_\infty)$ diagrams around Pauli-Z quantum gates. This behavior is associated with the complex component of the left-handed circular polarization of the initial state of the walker, which gives opposite signals for $\theta < \pi/2$ and $\theta > \pi/2$ for the dynamical evolution protocol due to acquisition of the intensity-dependent (nonlinear) phase described in Eq. (4). This statement becomes more evident when we show results obtained by employing the same methodology used earlier on the condition in which the initial state of the walker is given by $|\Psi(0)\rangle = |R\rangle \otimes |n_0\rangle$ (see Fig. 6). In general, the phenomenology is homologous, with normalized $\overline{\mathrm{IPR}}(t_\infty)$ and $\overline{\mathrm{SP}}(t_\infty)$ diagrams exhibiting the same regimes, but with the symmetric profile around $\theta = \pi/2$. Now the regime of stationary self-trapped quantum walks is even more concentrated around $\theta = \pi/2$.

IV. CONCLUSION

In summary, we have studied the dynamics of quantum walkers in nonlinear DTQWs. By considering a Kerr-like nonlinearity, we associated the acquisition of an intensity-dependent phase with the walker while it propagates on the lattice. With the nonlinear strength of the medium as an adjustable parameter, we explored the role of quantum gates in the emergence of mobile solitonlike structures and quantum walker dynamics, as well as the regime in which the quantum walker exhibits a localization induced by self-trapping. In the latter the dispersive mode is fully suppressed by nonlinearity, making the walker strongly trapped in the initial position, developing a breathing mode. The stationary self-trapped regime becomes predominant as θ gets closer to Pauli-Z quantum gates. We also have shown that the threshold between delocalized and localized regimes exhibits an unusual aspect in which an increment of the nonlinear parameter can induce the transition of the system from a localized to a delocalized regime. To conclude, by considering that nonlinearity has attracted much attention in quantum information science [37,53–55], we hope that our work may impel further investigations on quantum walks in nonlinear optical media. From an experimental point of view, we consider optical systems as the most promising in the implementation of our study. We suggest the use of Kerr-like optical media in the optical paths of experimental settings able to exhibit optical DTQWs, such as in a linear cavity [44], optical rings [45–47], a Michelson interferometer [48], or optical lattices [49].

ACKNOWLEDGMENTS

This work was partially supported by CNPq (Brazilian National Council for Scientific and Technological Development), CAPES (Federal Brazilian Agency), and FAPEAL (Alagoas State Agency).

[1] D. Hennig and G. Tsironis, Phys. Rep. **307**, 333 (1999).
[2] M. Fleischhauer, A. Imamoglu, and J. P. Marangos, Rev. Mod. Phys. **77**, 633 (2005).
[3] F. Lederer, G. I. Stegeman, D. N. Christodoulides, G. Assanto, M. Segev, and Y. Silberberg, Phys. Rep. **463**, 1 (2008).
[4] A. S. Davydov, *Solitons in Molecular Systems, Mathematics and Its Applications* (Springer Netherlands, Dordrecht, 1985).
[5] A. Scott, Phys. Rep. **217**, 1 (1992).
[6] F. Dalfovo, S. Giorgini, L. P. Pitaevskii, and S. Stringari, Rev. Mod. Phys. **71**, 463 (1999).
[7] Y. V. Kartashov, B. A. Malomed, and L. Torner, Rev. Mod. Phys. **83**, 247 (2011).
[8] O. Morsch and M. Oberthaler, Rev. Mod. Phys. **78**, 179 (2006).
[9] T. D. Holstein, Ann. Phys. (NY) **8**, 325 (1959).
[10] T. D. Holstein, Ann. Phys. (NY) **8**, 343 (1959).
[11] W. P. Su, J. R. Schrieffer, and A. J. Heeger, Phys. Rev. Lett. **42**, 1698 (1979).
[12] A. J. Heeger, S. Kivelson, J. R. Schrieffer, and W. P. Su, Rev. Mod. Phys. **60**, 781 (1988).
[13] H. A. Haus and W. S. Wong, Rev. Mod. Phys. **68**, 423 (1996).
[14] V. I. Kruglov and J. D. Harvey, Phys. Rev. A **98**, 063811 (2018).
[15] A. Hause, C. Mahnke, and F. Mitschke, Phys. Rev. A **98**, 033814 (2018).
[16] T. J. Kippenberg, A. L. Gaeta, M. Lipson, and M. L. Gorodetsky, Science **361**, eaan8083 (2018).
[17] A. R. C. Buarque and W. S. Dias, Commun. Nonlinear Sci. Numer. Simul. **63**, 365 (2018).
[18] A. J. Heeger, Rev. Mod. Phys. **73**, 681 (2001).
[19] E. J. Meier, F. A. An, and B. Gadway, Nat. Commun. **7**, 5382 (2016).
[20] J. J. Liu, Z. J. Wei, Y. L. Zhang, Y. Meng, and B. Di, J. Phys. Chem. B **121**, 2366 (2017).
[21] R. Y. Chiao, E. Garmire, and C. H. Townes, Phys. Rev. Lett. **13**, 479 (1964).
[22] S. F. Mingaleev and Y. S. Kivshar, Phys. Rev. Lett. **86**, 5474 (2001).
[23] Y. Chen, Opt. Lett. **16**, 4 (1991).
[24] A. S. Reyna, G. Boudebs, B. A. Malomed, and C. B. de Araújo, Phys. Rev. A **93**, 013840 (2016).
[25] M. A. Porras, Opt. Express **26**, 19606 (2018).
[26] C. A. Bustamante and M. I. Molina, Phys. Rev. B **62**, 15287 (2000).
[27] W. S. Dias, M. L. Lyra, and F. A. B. F. de Moura, Phys. Rev. B **82**, 233102 (2010).
[28] K. Nakata, K. A. van Hoogdalem, P. Simon, and D. Loss, Phys. Rev. B **90**, 144419 (2014).
[29] A. L. S. Pereira, M. L. Lyra, F. A. B. F. de Moura, A. R. Neto, and W. S. Dias, Commun. Nonlinear Sci. Numer. Simul. **64**, 89 (2018).
[30] C. Navarrete-Benlloch, A. Pérez, and E. Roldán, Phys. Rev. A **75**, 062333 (2007).

[31] Y. Shikano, T. Wada, and J. Horikawa, Sci. Rep. **4**, 4427 (2014).
[32] C.-W. Lee, P. Kurzyński, and H. Nha, Phys. Rev. A **92**, 052336 (2015).
[33] Y. Gerasimenko, B. Tarasinski, and C. W. J. Beenakker, Phys. Rev. A **93**, 022329 (2016).
[34] A. D. Verga, Eur. Phys. J. B **90**, 41 (2017).
[35] I. Vakulchyk, M. V. Fistul, Y. Zolotaryuk, and S. Flach, Chaos **28**, 123104 (2018).
[36] I. Vakulchyk, M. V. Fistul, and S. Flach, Phys. Rev. Lett. **122**, 040501 (2019).
[37] W.-C. Gao, C. Cao, X.-F. Liu, T.-J. Wang, and C. Wang, OSA Continuum **2**, 1667 (2019).
[38] Y. Aharonov, L. Davidovich, and N. Zagury, Phys. Rev. A **48**, 1687 (1993).
[39] M. A. Nielsen and I. L. Chuan, *Quantum Computation and Quantum Information* (Cambridge University Press, Cambridge, 2000).
[40] N. Shenvi, J. Kempe, and K. B. Whaley, Phys. Rev. A **67**, 052307 (2003).
[41] A. M. Childs, Phys. Rev. Lett. **102**, 180501 (2009).
[42] G. Di Molfetta, F. Debbasch, and M. Brachet, Phys. Rev. E **92**, 042923 (2015).
[43] C. M. Chandrashekar, R. Srikanth, and S. Banerjee, Phys. Rev. A **76**, 022316 (2007).
[44] P. L. Knight, E. Roldán, and J. E. Sipe, Phys. Rev. A **68**, 020301 (2003).
[45] P. L. Knight, E. Roldán, and J. Sipe, Opt. Commun. **227**, 147 (2003).
[46] P. L. Knight, E. Roldán, and J. Sipe, Opt. Commun. **232**, 443 (2004).
[47] A. Schreiber, K. N. Cassemiro, V. Potoček, A. Gábris, P. J. Mosley, E. Andersson, I. Jex, and C. Silberhorn, Phys. Rev. Lett. **104**, 050502 (2010).
[48] D. Pandey, N. Satapathy, M. S. Meena, and H. Ramachandran, Phys. Rev. A **84**, 042322 (2011).
[49] A. Crespi, R. Osellame, R. Ramponi, V. Giovannetti, R. Fazio, L. Sansoni, F. D. Nicola, F. Sciarrino, and P. Mataloni, Nat. Photon. **7**, 322 (2013).
[50] P. K. Datta and A. M. Jayannavar, Phys. Rev. B **58**, 8170 (1998).
[51] X.-P. Xua, Eur. Phys. J. B **77**, 479 (2010).
[52] A. R. C. Buarque and W. S. Dias, Phys. Rev. E **100**, 032106 (2019).
[53] J. H. Shapiro, Phys. Rev. A **73**, 062305 (2006).
[54] D. J. Brod and J. Combes, Phys. Rev. Lett. **117**, 080502 (2016).
[55] A. Nysteen, D. P. S. McCutcheon, M. Heuck, J. Mørk, and D. R. Englund, Phys. Rev. A **95**, 062304 (2017).